Phase Behavior and Block Sequence Effects in Lithium Perchlorate-Doped Poly(isoprene-*b*-styrene-*b*-ethylene oxide) and Poly(styrene-*b*-isoprene-*b*-ethylene oxide) Triblock Copolymers

Thomas H. Epps, III, Travis S. Bailey, Ryan Waletzko, and Frank S. Bates*

Department of Chemical Engineering and Materials Science, University of Minnesota, Minneapolis, Minnesota 55455

Received July 29, 2002

ABSTRACT: We compare the phase behavior of a series of lithium perchlorate-doped poly(isoprene-*b*-styrene-*b*-ethylene oxide) (ISO) and poly(styrene-*b*-isoprene-*b*-ethylene oxide) (SIO) triblock copolymers. Complete phase diagram isopleths ($f_I = f_S$) are described for the lithium-doped ISO system and the previously reported lithium-doped SIO system. We examine the effects of block sequencing on the microstructures present in the doped SIO and ISO diagrams using small-angle X-ray scattering. Three phases were identified in the doped ISO phase diagram isopleth: two-domain lamellae (LAM_2), core−shell cylinders (CSC), and three-domain lamellae (LAM_3). The order−disorder transition temperatures increase dramatically upon doping and salt loadings up to [O]:[Li] concentrations of 3:1 are accomplished without macrophase separation. The increase in segregation strength in the ISO system upon doping leads to a disappearance of the more geometrically elaborate network phase in favor of the CSC phase as a result of the imbalance in interaction parameters. In addition, we used differential scanning calorimetry (DSC) to determine the effect of having either a glassy block or a rubbery block adjacent to the poly(ethylene oxide) (PEO) block in both neat and doped samples. Melting temperatures for a given domain thickness are lower in the ISO triblock copolymers relative to the SIO counterparts. This temperature discrepancy is associated with confinement by the glassy polystyrene block, which reduces the crystallite size, leading to PEO melting temperatures that are closer to room temperature in ISO triblock copolymers. Through comparative phase diagram and DSC studies, we have gleaned the effects of connectivity and lithium perchlorate concentration on triblock copolymer microstructure.

I. Introduction

ABC triblock copolymers offer a unique opportunity to create materials with exciting chemical and physical properties. In previous works, we described the characterization of a series of neat poly(styrene-*b*-isoprene-*b*-ethylene oxide) (SIO) triblock copolymers above the melting temperature of the poly(ethylene oxide) (PEO) block[1] and also following doping of the PEO block with various concentrations of lithium perchlorate.[2] As lithium perchlorate salt was added to the SIO triblock copolymer, the system was forced into a stronger segregation regime due to localization of the polar salt within the PEO domain. This increase in segregation strength upon doping was accompanied by increases in the domain spacing and order−disorder transition temperatures.[2−4] Consistent with the behavior reported in diblock copolymers, this enhanced segregation strength led to the elimination of the more geometrically complex, "nonclassical" structures along the phase diagram isopleth.[5−7] In the SIO system, we found that the core−shell gyroid (CSG) and semiperforated lamellar (SPL) phases were extinguished and replaced by the core−shell cylindrical (CSC) morphology. A summary of the neat and doped SIO phase diagrams is presented in Figure 1. The neat system exhibited six morphologies in the transition from a symmetric two-domain diblock to a symmetric three-domain triblock state, while the doped system showed only four. Also, the composition dependence of the order−disorder transition, $T_{ODT}(f_{PEO})$, changes qualitatively.

Dramatically different phase behavior was discovered in the neat poly(isoprene-*b*-styrene-*b*-ethylene oxide) (ISO) system, which we attributed to the elimination of the chain packing frustration condition present in the SIO system.[8] In this case, the two least compatible blocks, PI and PEO, are not chemically connected, resulting in just one ordered phase between two-domain and three-domain lamellae (LAM_2 and LAM_3), tentatively identified as a co-continuous noncubic network structure. The corresponding phase diagram is shown in Figure 2a.

This article focuses on the effects of doping the ISO triblock copolymers with lithium perchlorate. Our goals are twofold: first to evaluate the effects of salt doping on the overall melt phase behavior and second to establish the role of block sequencing on the crystallization of PEO within the confined microdomains near room temperature. Both aspects of this study are relevant to the application of PEO-containing block copolymers as electrolytes.[4]

The majority of the literature on PEO conductivity has focused on increasing ion transport in the amorphous material, and the crystalline material is thought to significantly reduce conductivity. Thus, the many studies have focused on the reduction of crystalline material in polymer electrolytes.[9−17] Recently, Gajourova et al. and Golodnitsky and co-workers have reported greater ionic conductivities in crystalline PEO[18] and PEO materials where the chains are aligned through stretching.[19,20] In either case, understanding the role of block sequence and salt doping on crystallite formation is important in the creation of a polymer electrolyte.

Previous publications on confinement in polymer systems have shown that placement of a glassy block or a rubbery block adjacent to a crystallizable block can

* To whom correspondence should be addressed.

10.1021/ma021231o CCC: $25.00
Published on Web 03/19/2003

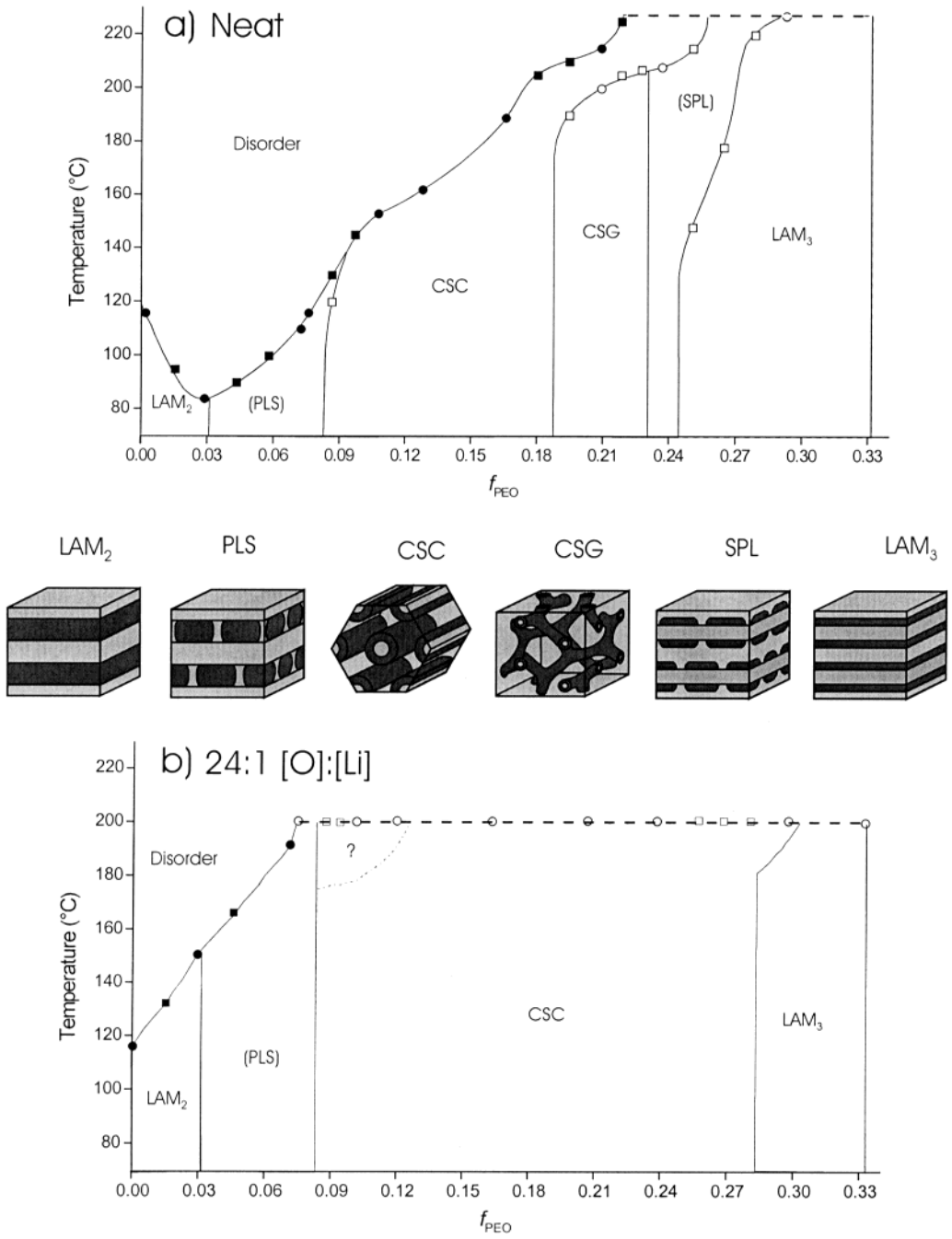

Figure 1. (a) Neat SIO phase diagram adapted from Bailey et al. detailing the structures found along the $f_S = f_I$ isopleth.[1] (●) and (■) represent T_{ODT} for neat triblock samples and blends, respectively. (○) and (□) represent order−order transitions in triblock samples and blends, respectively. The dashed horizontal line at 225 °C identifies the highest experimental temperature. (b) Phase diagram detailing the structures found in the lithium-doped SIO triblock isopleth. (●) and (■) represent ODTs for triblock samples and blends, respectively. (○) and (□) represent locations of triblock samples and blends, respectively, at the experimental ceiling.

influence crystallite formation.[21−27] Lee and co-workers found that in a block copolymer melt crystallization sometimes perturbed the microstructure depending on the glass transition temperature (T_g) of the amorphous block.[26] Weimann and others reported that the size of the confined crystallizable domain directly influenced the sample's crystallite size and melting temperature.[23,24] Hamley and Floudas have studied the effects of PEO crystallization in diblock copolymers with both PI[28,29] and poly(oxybutylene),[29] noting the confining effects of the hard poly(oxybutylene) block vs the soft PI block. However, to the authors' knowledge, Hamley and Floudas have not investigated PEO confinement effects in polymers containing both a hard and soft amorphous block. The efficacy of lithium-doped PEO as an ionic conductor is inextricably coupled to the state of crystallinity. Triblock copolymers offer a potentially useful strategy for optimizing lithium mobility through the reduction of crystallinity due to confinement and control over microdomain geometry. This work addresses the optimization strategy through a greater understanding of the influence of lithium perchlorate on triblock phase behavior and block interaction.

II. Experimental Section

Synthesis and Characterization of Poly(isoprene-*b*-styrene-*b*-ethylene oxide) (ISO) Triblock Copolymers. ISO triblock copolymers were synthesized using sequential

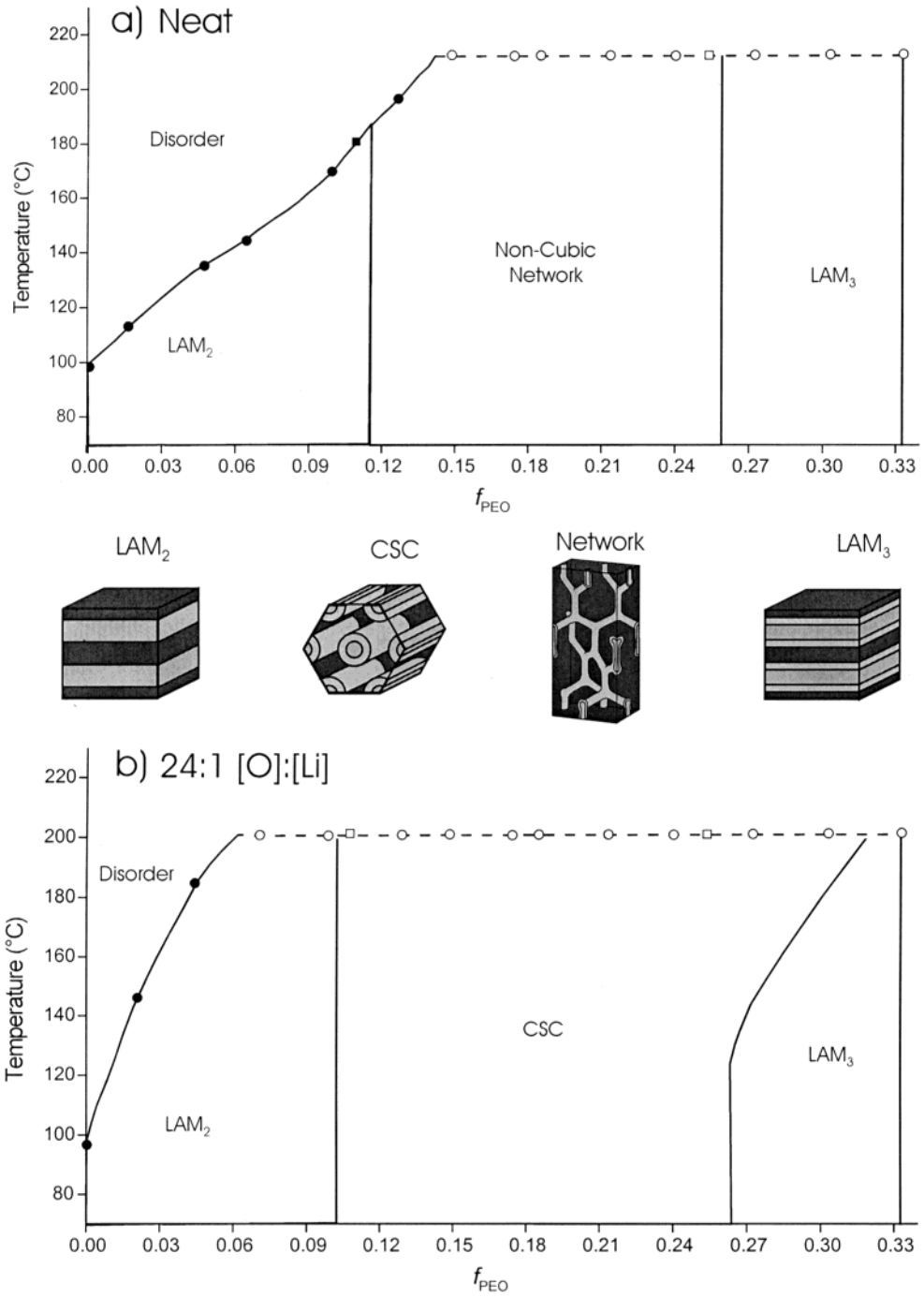

Figure 2. (a) Neat phase diagram from ref 8 detailing the structures located in the ISO triblock copolymer phase diagram isopleth. (●) and (■) represent ODTs for triblock samples and blends, respectively. (○) and (□) represent locations of triblock samples and blends, respectively, at the experimental ceiling. The dashed horizontal line at 200 °C represents the experimental ceiling. (b) Doped phase diagram detailing the structures found in the lithium-doped ISO triblock copolymer phase diagram isopleth. Symbol notation is same as in Figure 2a.

anionic polymerization techniques. Initial polymerization steps required the synthesis of a poly(isoprene-*b*-styrene) (IS) diblock end-capped with a single hydroxyl group. Subsequently, a series of ISO triblocks was produced by reinitiation of the diblock with potassium naphthalenide and addition of ethylene oxide. In this way, 13 ISO triblocks were created with PEO volume fractions ranging from 0% to 34.1%. Copolymer compositions were determined by NMR, and repeat unit mole fractions were calculated on the basis of relative peak intensities with volume fractions calculated on the basis of published homopolymer densities at 140 °C;[30] the associated PEO weight and volume fractions (w_{PEO} and f_{PEO}) are listed in Table 1. Two binary blends, denoted ISO*i*/*j*, where ISO*i* and ISO*j* are the constituents, are also identified in Table 1. Density data were not corrected to reflect differences in temperature. Detailed descriptions of the synthesis, characterization, and blending procedures can be found in Bailey et al.[1]

Lithium Perchlorate Doping. Lithium perchlorate was obtained from Aldrich (99.5%) and used as received. A measured amount of triblock copolymer and salt was dissolved in THF. Samples were freeze-dried in either 2 mL ampules or 10 mL vials and stored under vacuum prior to use. To eliminate the possibility of solvent induced morphological differences, the neat polymer specimens were subjected to the same treatment.

Small-Angle X-ray Scattering (SAXS). SAXS experiments were conducted at the University of Minnesota Institute of Technology (IT) characterization facility. Cu Kα X-rays (1.54

Table 1. Phase Behavior of Poly(isoprene-*b*-styrene-*b*-ethylene oxide)/$LiClO_4$ Mixtures

sample[a]	w_{PEO}	f_{PEO}	ODT[b] (°C)	[O]:[Li] = 48:1 morphology[c]	ODT[b] (°C)	[O]:[Li] = 24:1 morphology[c]
parent diblock[d]	0.003	0.003	97	$LAM_2 \rightarrow$ DIS	97	$LAM_2 \rightarrow$ DIS
ISO1	0.019	0.019	123	$LAM_2 \rightarrow$ DIS	143	$LAM_2 \rightarrow$ DIS
ISO5	0.054	0.049	155	$LAM_2 \rightarrow$ DIS	182	$LAM_2 \rightarrow$ DIS
ISO2	0.073	0.065	200	$LAM_2 \rightarrow$ DIS		LAM_2
ISO3	0.111	0.098		LAM_2		LAM_2
ISO3/4	0.122	0.108		LAM_2		CSC
ISO4	0.141	0.125		CSC		CSC
ISO7	0.170	0.150		CSC		CSC
ISO13	0.200	0.177		CSC		CSC
ISO6	0.207	0.183		CSC		CSC
ISO8	0.238	0.211		CSC		CSC
ISO9	0.268	0.239		CSC		CSC
ISO9/10	0.280	0.250		CSC		CSC
ISO10	0.303	0.271		$LAM_3 \rightarrow$ CSC		$LAM_3 \rightarrow$ CSC
ISO11	0.335	0.301		LAM_3		$LAM_3 \rightarrow$ CSC
ISO12	0.378	0.341		LAM_3		LAM_3

[a] The notation ISO*i*/*j* represents a blend made from polymers ISO*i* and ISO*j*. [b] An unlisted ODT indicates that the transition temperature is greater than 200 °C. [c] DIS = disordered state; LAM_2 = two-domain lamellae; CSC = hexagonal core−shell cylinders; LAM_3 = three-domain lamellae. [d] The molecular weight of the parent diblock is 13 500 g/mol.

Å) were generated using a Rigaku RU-200BVH rotating anode equipped with a 0.2 × 2 mm microfocus cathode and total reflecting Franks mirror optics. 2D-SAXS data were collected by a Siemens HI-STAR multiwire area detector. All SAXS data presented in this report were corrected for detector response characteristics and plotted on a logarithmic scattering intensity axis vs the magnitude of the scattering vector, $|\mathbf{q}|$,

$$|\mathbf{q}| = q = \frac{4\pi}{\lambda}\sin\left(\frac{\theta}{2}\right)$$

Dynamic Mechanical Spectroscopy (DMS). Mechanical spectroscopy experiments were conducted on a Rheometrics Scientific ARES strain-controlled rheometer using a parallel plate configuration with 25 mm diameter plates. Isochronal (ω = 1 rad/s) temperature ramps at a constant heating rate (between 1 and 6 °C/min) were employed to measure the dynamic elastic (G') and loss (G'') moduli.

DMS was an important tool in the determination of phase boundaries, indicating the locations of both order−order and order−disorder transitions. All T_{ODT} values presented in this report were obtained from heating runs, and each run was repeated to ensure that the sudden drop in elastic moduli was caused by a phase transition to a disordered state, not polymer degradation. The order−order and order−disorder transition data were corroborated by SAXS measurements. A more detailed description of DMS procedures is presented in a previous publication.[2]

Differential Scanning Calorimetry (DSC). Calorimetry experiments were conducted on a Perkin-Elmer Pyris 1 differential scanning calorimeter with a Cryofill liquid nitrogen attachment. DSC allowed for the determination of melting temperatures and percent crystallinity of the triblock samples. Isobaric temperature ramps at constant heating rate (between 10 and 20 °C/min) were conducted to measure the heat input requirements. Sample melting points were associated with well-defined peaks in the heat input requirement. The percent crystallinity was determined by calculating the area under the melting peaks and referencing to the heat of fusion of bulk PEO (213 J/g).[15]

Samples were stored in sealed containers at 0 °C for at least 2 weeks prior to use. Immediately before use, the sealed samples were allowed to thermally equilibrate at room temperature before a measured amount (between 3.5 and 6.5 mg) was sealed in a 0219-0041 aluminum pan. The system was cooled to −60 °C and allowed to thermally equilibrate prior to performing temperature scans. A heating scan was run up to 200 °C, followed by a cooling scan to −60 °C. First and second heating and cooling cycles were applied to all samples. Runs were repeated after samples had been stored at 0 °C for at least 2 more weeks to ensure reproducibility.

III. Results and Analysis

IIIA. Melt State Effects of Lithium Perchlorate. ISO triblock copolymers were doped at main-chain oxygen-to-lithium ratios ([O]:[Li]) ranging from 48:1 to 3:1. Several specimens with intermediate PEO contents were made by blending adjacent triblocks prior to the addition of salt. The remainder of this section is divided into five parts, discussing different aspects of the characterization experiments above the melting temperature of PEO.

Order−Disorder Transition (ODT). Order−disorder transition temperatures (T_{ODT}) were determined by dynamic mechanical spectroscopy (DMS) and small-angle X-ray scattering (SAXS) based on well-documented procedures.[1,2] Results for [O]:[Li] ratios of 48:1 and 24:1 are listed in Table 1. T_{ODT} values were accessible only at the lowest PEO compositions since measurements were not extended above 200 °C. In all cases addition of salt elevated T_{ODT} as illustrated in Figure 2.

Polymer Morphology as a Function of PEO Volume Fraction. Changes in PEO volume fraction affected the polymer morphologies of the lithium-doped ISO triblock copolymers. Sample SAXS traces of the various detected morphologies are shown in Figure 3. Figure 3a (upper panel) shows results for a neat ISO5 (4.9 % PEO by volume) sample at 100 °C. The single peak is characteristic of the two-domain lamellar morphology (LAM_2) and was verified through TEM analysis.[8] Higher-order peaks were not detected. The SAXS pattern from the 24:1 doped ISO5 specimen at 100 °C is shown in Figure 3a (lower panel). Again, only a single peak was detected. For the 24:1 doped system, the LAM_2 region spans from 0 to 10.3% PEO by volume.

Figure 3b (upper panel) shows results for the neat ISO6 (18.3% PEO by volume) sample at 120 °C. The SAXS pattern is identical to that of the tentatively identified co-continuous noncubic network structure.[8] The corresponding SAXS pattern for the 24:1 doped ISO6, sample shown in the lower panel of Figure 3b (also at 120 °C), exhibits distinct Bragg peaks located at q^*, $\sqrt{3}q^*$, $\sqrt{4}q^*$, $\sqrt{7}q^*$, and $\sqrt{9}q^*$ (not shown) indicative of a hexagonal core−shell cylindrical (CSC) morphology. In addition, the relative peak locations and intensities match theoretical predictions of a CSC phase where cylindrical PEO cores are encased in PS shells,

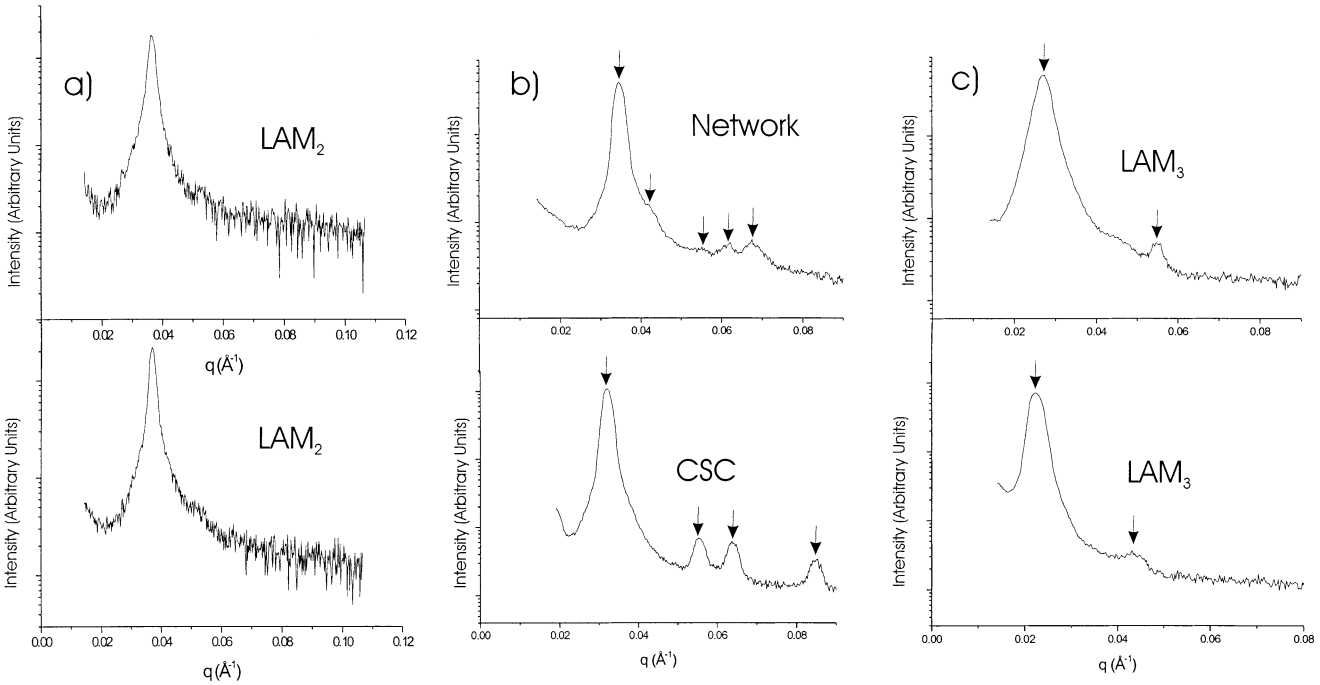

Figure 3. Representative SAXS patterns obtained from neat (upper curves) and doped 24:1 (lower curves) ISO specimens: (a) ISO5 at 100 °C; (b) ISO6 at 120 °C; (c) ISO11 at 140 °C.

surrounded by a PI matrix. For the 24:1 lithium-doped system, SAXS analysis as a function of composition and temperature revealed that the CSC region occurs between 10.3 and 26.4% PEO by volume (see Table 1).

Figure 3c (upper panel) shows an example SAXS pattern for a neat ISO11 (30.1% PEO by volume) sample at 140 °C. The two detected peaks at q^* and $2q^*$ are consistent with a three-domain lamellar (LAM_3) morphology. This result was confirmed by TEM analysis (not shown). SAXS data from the 24:1 lithium-doped ISO11 sample obtained at 140 °C (lower panel of Figure 3c) show a similar pattern. From this and similar experiments we conclude that the 24:1 samples contain the LAM_3 morphology over the composition range from 26.4 to 34.1% PEO by volume. PEO compositions extending past the symmetric triblock were not studied in this investigation.

Polymer Morphology as a Function of Salt Concentration. As with the SIO system,[2] the stability of the phase diagram was evaluated at salt concentrations spanning the optimal conductivity range for lithium perchlorate in PEO. Figure 4a,b shows representative SAXS patterns at 140 °C as a function of concentration for ISO13 (17.7% PEO by volume). Figure 4a presents the first-order (q^*) peaks while Figure 4b highlights the higher-order diffraction peaks. The stability of the CSC phase in this polymer is evidenced by the persistence of the characteristic scattering peaks up to a 3:1 salt concentration. (The neat sample exhibits the proposed noncubic network structure.) The peak resolution is only modestly affected by salt concentration; however, a dramatic shift in peak locations to lower q values is evident as the salt concentration increases as shown in Figure 4c. For the CSC structure, the first allowed reflection derives from the d_{100} lattice spacing. Simple ideal volumetric mixing of the lithium perchlorate salt and PEO would produce a marginal increase in the calculated lattice spacing with increasing salt content as indicated by the open symbols in Figure 4c. However, the experimental SAXS data exhibit a marked increase in the d_{100} spacing as the [O]:[Li] ratio rises from 48:1 to 3:1. At the 3:1 concentration, the domain spacing is approximately 60% greater than for the ideally mixed system.

Consistent with previous work,[2] the 1:1 samples showed complete disruption of the phases present at lower salt concentrations and were not investigated in detail because this salt concentration is significantly higher than that necessary for optimal conductivity.[31−33]

Polymer Morphology as a Function of Temperature. The effects of temperature on polymer morphology were studied by SAXS between 70 and 200 °C for ISO4 specimens from 48:1 to 3:1. Heating and cooling runs produced nearly identical SAXS results in all cases consistent with the CSC morphology; minor shifts in the Bragg peak locations toward higher q values occurred with heating.

Lithium-Doped ISO Phase Diagram Isopleth. Lithium-doped phase diagram isopleths were constructed on the basis of the SAXS and DMS analysis of 13 ISO triblock copolymers and two ISO triblock blends. By varying PEO volume fraction, temperature, and $LiClO_4$ concentration, we have constructed several pseudo-three-component phase diagrams at various [O]:[Li] ratios. A sample isopleth for the 24:1 salt composition is shown in Figure 2b. The upper limit of the experimental temperature range is indicated by a dashed line at 200 °C chosen to avoid polymer degradation, which becomes a concern above this temperature. The lower bound of our temperature range was 70 °C. Room temperature samples exhibited the same morphologies as samples at 70 °C as verified by room temperature SAXS and TEM measurements (not shown). The horizontal axis of Figure 2 represents the PEO volume fraction in the ISO triblock copolymer and runs from 0% PEO (parent IS diblock copolymer) to 34.1% PEO (symmetric triblock copolymer).

All lithium-doped phase diagrams contain three morphologies. In order of appearance, they are two-domain lamellae (LAM_2), hexagonally packed core−shell cylin-

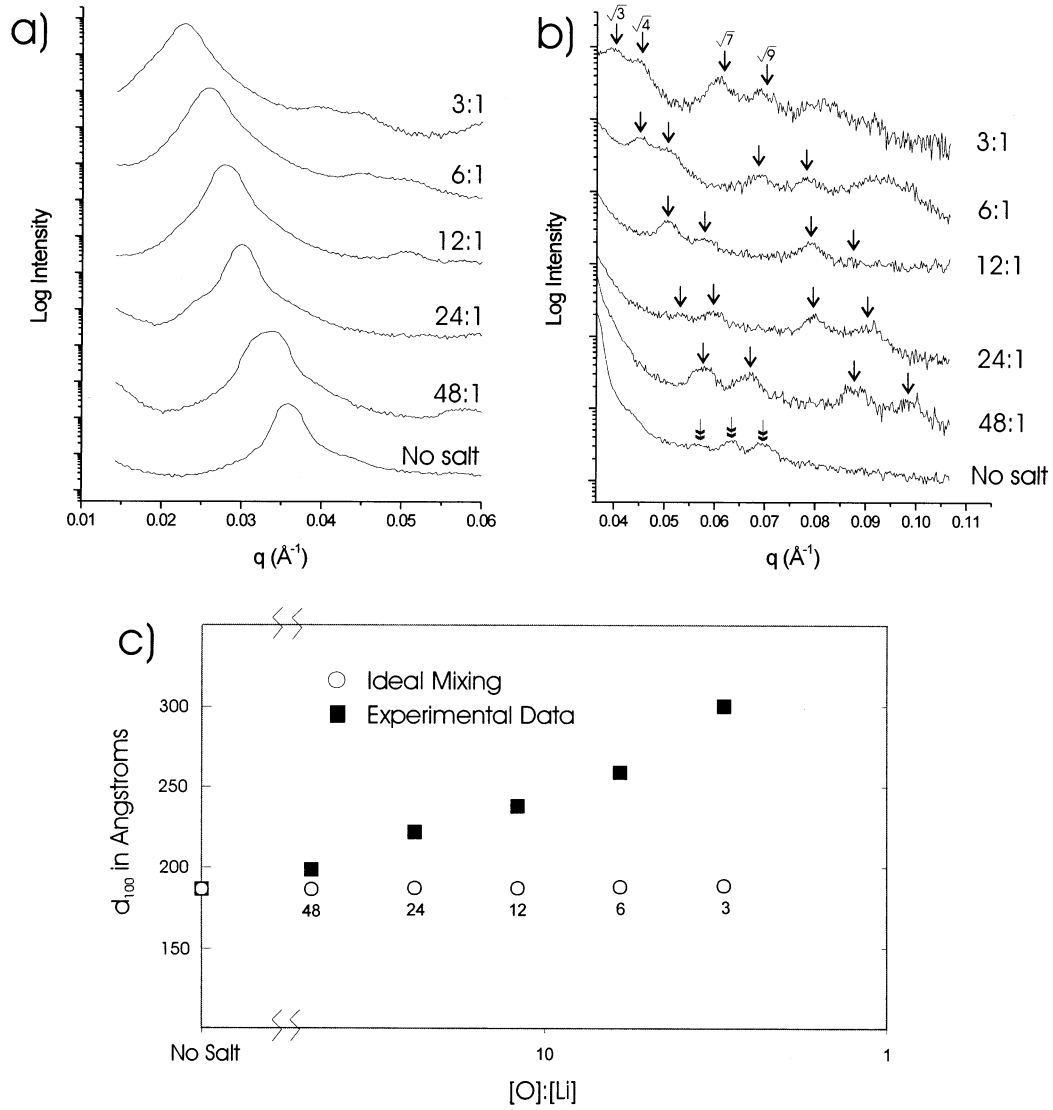

Figure 4. (a) $I(q)$ vs q SAXS results for various $LiClO_4$ concentrations in ISO13 at 140 °C. The first-order peak is highlighted to show the decrease in q^* as salt is added to the system. (b) $I(q)$ vs q SAXS results for samples shown in (a) with a q range of 0.04−0.11 Å^{-1}. The highlighted higher-order diffraction peaks are consistent with the core−shell cylinder (CSC) morphology (the no salt sample is a tentatively identified noncubic network morphology). Each scattering pattern was progressively shifted vertically. (c) Hexagonal CSC domain spacing, d_{100}, obtained from the SAXS data. (■) represents actual SAXS data. (○) represents the estimated domain spacing based on ideal volumetric mixing of PEO and $LiClO_4$. These results indicate considerable chain stretching in the salt mixtures.

ders (CSC), and three-domain lamellae (LAM_3). This differs from the neat ISO phase diagram depicted in Figure 2a, which includes LAM_2, a co-continuous network phase, and LAM_3. In the doped diagram (Figure 2b), the CSC phase replaces the network phase found in the neat materials. It is apparent that the system thermodynamics are affected by relatively small amounts of salt. A salt concentration of 48:1 provides enough of a change in the free energy balance to transform the most stable phase from the co-continuous network structure to the CSC phase. In addition, the CSC phase has noticeably encroached on the LAM_3 region on the right side of Figure 2b. Also, there is a small increase in the CSC region at the expense of the LAM_2 phase as a function of salt concentration on the left side of Figure 2b; however, this is a very modest increase (on the order of 1% when comparing the neat and 24:1 doped diagrams). This increase in the cylindrical region at the expense of the lamellar regions was documented in all the lithium-doped phase diagrams and appeared to increase as the salt concentration was raised. The only order−order transition (OOT) identified in the lithium-doped phase diagram isopleth was between the LAM_3 and CSC phases. As the salt concentration increased, this OOT shifted toward lower temperatures. The reduction of the OOT as a function of salt concentration again emphasizes the increased stability of the CSC phase in the doped system.

All lithium-doped phase diagram isopleths showed a dramatic increase in the experimentally accessible order−disorder transition temperatures upon doping. For example, in Figure 2, the ODT of ISO2 (6.5% PEO by volume) rises an estimated 60 °C when the neat material is doped to the moderate lithium concentration of 24:1. A similar trend of increasing ODTs was noted in all samples on a given isopleth.

IIIB. Block Sequence Effects on Crystallinity. This section addresses the effects of PEO confinement between glassy (PS) or rubbery (PI) domains in neat and $LiClO_4$-doped ISO and SIO triblock copolymers on polymer crystallinity. Initial heating and cooling traces for neat and lightly doped (48:1) SIO3 samples and neat

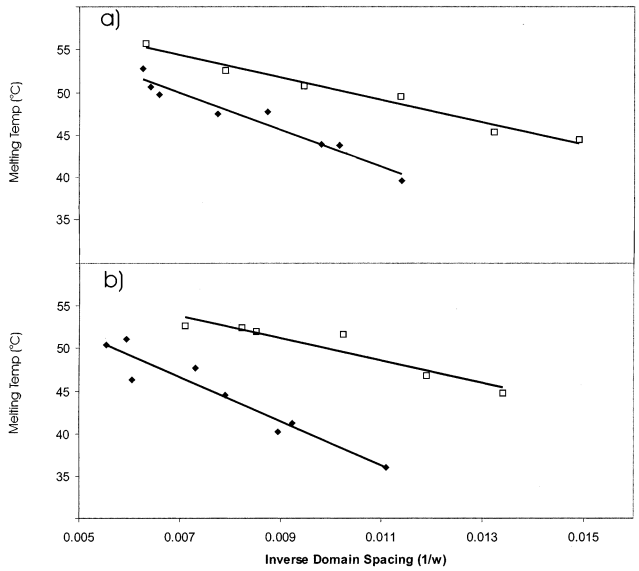

Figure 5. PEO melting temperature vs inverse PEO domain size ($1/w$) as a function of block architecture (□, SIO; ◆, ISO) and lithium doping. w is given in Å. (a) Neat compounds. (b) Lithium-doped (24:1) compounds. Melting temperatures were determined from DSC measurements. Linear fits to the data (solid lines) extrapolate to infinite PEO domain size (i.e., bulk PEO).

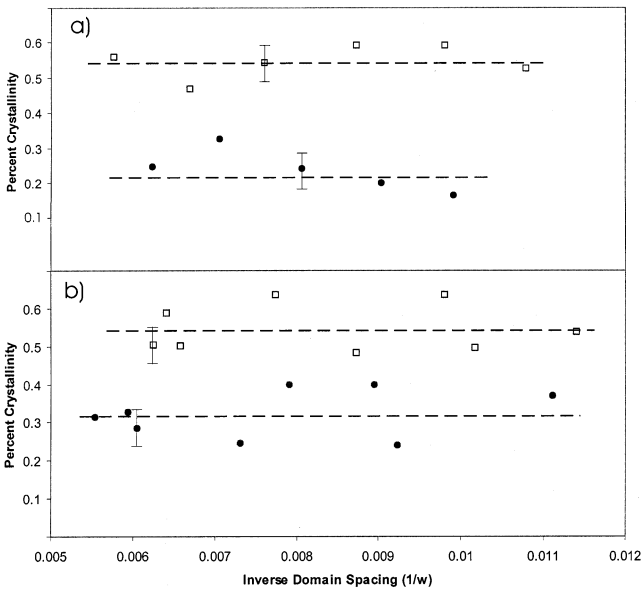

Figure 6. Percent PEO crystallinity vs inverse PEO domain size ($1/w$) as a function of block architecture and lithium doping at 48:1. w is given in Å. (a) SIO compounds (□, neat; ●, doped). (b) ISO compounds (□, neat; ●, doped). Percent crystallinity was calculated on the basis of DSC measurements assuming a heat of fusion of 213 J/g.[15]

and lightly doped (48:1) ISO7 samples showed melting peaks between 35 and 55 °C upon heating, and most exhibited recrystallization endotherms upon cooling. Triblock samples doped with intermediate salt concentrations, such as 12:1 and 6:1, produced no discernible melting or crystallization peaks in the DSC traces. This agrees with the works of Watanabe and others, who explained that slow crystallization kinetics near the eutectic point (approximately 10:1) and the reduction of chain mobility due to the increased glass transition temperature led to an absence of melting or crystallization peaks.[11,34,35] DSC traces for the 3:1 samples exhibited melting peaks at approximately 150 °C corresponding well to the melting temperature of the bulk PEO/$LiClO_4$ 3:1 complex reported by Robitaille and Fauteux.[31] Henderson showed that faster crystallization kinetics exhibited in the formation of the 3:1 crystal structure led to the melting peaks found in our samples.[35]

PEO Melting Temperature as a Function of PEO Domain Size and Block Sequence. The influence of domain spacing on melting temperature was studied in the SIO and ISO systems for the neat and lightly doped (48:1) materials. Figure 5a displays PEO melting point data for the neat SIO and ISO compounds. In both cases, a linear correlation was obtained between melting temperature and inverse PEO domain size in angstroms, $1/w$, consistent with prior studies that link microdomain confinement and crystallite size to melting temperature.[23,24,36,37] One interesting trend in Figure 5a is that the melting temperatures of the ISO samples at a given domain size are all significantly lower than the SIO counterparts. At a PEO domain size of approximately 87 Å ($1/w = 0.0115$), the difference in melting temperature between the SIO and ISO samples is 12 °C. This difference decreases as the domain size increases; for example, at a domain spacing of approximately 160 Å ($1/w = 0.006\,25$), the difference in melting temperatures is just 4 °C. In the SIO and ISO samples the extrapolated melting temperatures at infinite domain size are approximately 65 °C, the accepted melting temperature of bulk PEO.[14,15,31,38] A similar trend was recorded for the 48:1 (Figure 5b) and 24:1 doped samples. Here again, the melting temperatures of the ISO samples at a given PEO domain size are significantly lower than the SIO counterparts, yet extrapolation to infinite PEO domain size gives approximately 64 °C, which is close to the melting temperature of bulk doped (48:1) PEO.[31]

PEO Percent Crystallinity as Function of PEO Domain Size and Block Sequence. Percent PEO crystallinity (obtained by integrating the melting endotherms) also was evaluated as a function of $1/w$ as presented in Figure 6. Similar results were obtained for the neat and doped SIO (Figure 6a) and neat and doped ISO (Figure 6b) materials. In all cases the percent crystallinity is independent of domain spacing and block sequence within experimental error. However, 48:1 doping reduces the average degree of PEO crystallinity from approximately 54% to 30% (the average percent crystallinity for bulk PEO is approximately 65%−70% under similar conditions).[15] We note that the LAM_2 samples, which showed marked reductions in percent crystallinity due to mixing of the PS and PEO blocks,[8] are not included in these figures.

IV. Discussion

It is well-known that $LiClO_4$ can be mixed in moderate amounts with PEO.[15,16,33,34] Our experiments suggest that salt loadings up to those reported for pure PEO can be obtained in this triblock copolymer system. Figure 4 indicates that the CSC morphology is stable over the entire doping range from 48:1 to 3:1. Thus, we believe that nanoscale domain formation does not hinder the doping of block copolymers to optimal conductivity levels. This agrees with results obtain in several previous works.[2,4]

Perhaps the most striking effect associated with salt doping is the loss of phase complexity in both the SIO and ISO systems (see Figures 1 and 2), which we attribute to the modification of the interaction param-

eters between blocks. Because $LiClO_4$ selectively partitions into the PEO domains, the PS/PEO and PI/PEO interaction parameters (χ_{SO} and χ_{IO}) must increase dramatically, thereby shifting the delicate balance of factors that control domain type and dimension. In the strong segregation regime for diblock copolymers, theory and experiment indicate $d^* \sim \chi^{1/6}$,[39−41] where d^* is the principal domain spacing. Crudely applying this relationship to the ISO triblock system, an overall interaction parameter (χ_{eff}) can be estimated as a function of salt concentration in the PEO block. For the 3:1 ISO system $\chi_{eff} \approx 17.1\chi$, while for the 24:1 system, $\chi_{eff} \approx 2.4\chi$, where χ is the overall interaction parameter for the nondoped system (i.e., $\chi_{eff} = \chi$ for the no salt case). Similarly for SIO, we find $\chi_{eff} \approx 9.1\chi$ and $\chi_{eff} \approx 1.4\chi$ for the 3:1 and 24:1 salt loadings, respectively. The greater impact of salt on the ISO vs the SIO system can be rationalized on the basis of the interaction parameters described as a function of temperature by the following equations:[42]

$$\chi_{SO} = \frac{29.8}{T} - 22.9 \times 10^{-3}$$

$$\chi_{IO} = \frac{90.0}{T} - 57.9 \times 10^{-3}$$

$$\chi_{SI} = \frac{26.4}{T} - 2.9 \times 10^{-3}$$

For the undoped material $\chi_{SO} \cong 0.05$ and $\chi_{IO} \cong 0.18$ at 100 °C; $\chi_{IS} \cong 0.07$ at this temperature, and we will assume χ_{IS} is unaffected by $LiClO_4$ doping. This distribution of segment−segment interactions produces a fascinating mix of morphologies as a function of PEO content, as evident in Figures 1a and 2a. Addition of $LiClO_4$ to PEO distorts the delicate balance between χ_{IS}, χ_{IO}, and χ_{SO} by greatly increasing the polarity (and presumably the solubility parameter) of the PEO domains, which elevates the interfacial tension between PEO and PI, and PEO and PS, thus favoring a reduction in the overall PEO interfacial area which necessitates additional chain stretching (i.e., inflation in d^*). As a consequence, the core−shell cylinder structure becomes the dominant morphology. Once the PS/PEO or PI/PEO interfacial tension dominates the overall free energy balance, the other interactions become relatively unimportant. We believe it is primarily this imbalance in the magnitude of χ's that creates a single CSC morphology regardless of block sequencing.

Data acquired at and below the melting temperature of the PEO block indicate that microphase separation and block sequencing do influence the crystallization behavior in these materials. Microdomain confinement leads to melting point depression in SIO and ISO triblocks, in both the neat and $LiClO_4$-doped specimens. Modest levels of doping appear to have no effect on T_m; however, doping does drastically reduce the fraction of crystalline PEO (Figure 6). From these results we conclude that crystallite size is controlled in part by d^* (as shown earlier with hydrocarbon block copolymers),[23,24] and the reduction of the percent crystallinity seems to reflect a local segregation of salt into amorphous regions, just as occurs with PEO homopolymer.

Figure 5 also reveals an important difference in T_m at all d^* between the SIO and ISO specimens. This could be attributed to two different factors. First, $\chi_{SO} < \chi_{IO}$, leading to a greater degree of interfacial mixing of PS with the PEO blocks. Alternatively, the glassy PS domains may offer more effective confinement than rubbery PI domains ($T_g \cong -60$ °C), thereby better suppressing crystallization. Since $LiClO_4$ doping does not seem to influence T_m (Figure 5), yet does greatly modify χ_{SO} and χ_{IO}, we conclude that this melting point reduction effect is attributable to hard vs soft wall confinement.

Even though T_m (hence the crystallite size) is effected by the connectivity of the triblock copolymer, the percent crystallinity is invariant (see Figure 6). This lends further credence to the argument that interblock mixing does not affect the crystallite size, as interblock mixing would reduce the percentage of crystallinity in the neat ISO system. This value is approximately 10−15% lower than the value normally associated with bulk PEO,[15] indicating that PEO confinement in a triblock morphology provides a significant reduction in crystallinity.

V. Conclusions

We have evaluated the roles of block sequencing and lithium perchlorate doping on the phase behavior of poly(styrene-*b*-isoprene-*b*-ethylene oxide) and poly(isoprene-*b*-styrene-*b*-ethylene oxide) triblock copolymers along the $f_I = f_S$ compositional isopleth from a parent diblock copolymer to the symmetric $f_I = f_S = f_O$ triblock copolymer. In the ISO system, lithium doping led to an increase in segregation strength as shown by the increase in order−disorder transition temperatures and domain spacings as determined by SAXS measurements. Doping at salt concentrations ranging from 48:1 to 3:1 ([O]:[Li]) transforms the proposed network phase in the ISO phase diagram to the core−shell cylindrical (CSC) morphology. Within the CSC phase $LiClO_4$ was dispersed in the PEO block up to a loading of 3:1 without inducing macroscopic phase separation. PEO confinement leads to a reduction in melting temperature that is not affected by light $LiClO_4$ doping. However, the melting temperature reduction for a given domain size is greater in the ISO relative to the SIO triblock copolymers. This enhancement is associated with PEO confinement between the hard, glassy PS microdomains.

Acknowledgment. This work was supported by the Lucent Technologies CRFP Fellowship Program and the NSF (DMR-0220460). The University of Minnesota MRSEC program is acknowledged for equipment support.

References and Notes

(1) Bailey, T. S.; Pham, H. D.; Bates, F. S. *Macromolecules* **2001**, *34*, 6994−7008.
(2) Epps, T. H.; Bailey, T. S.; Pham, H. D.; Bates, F. S. *Chem. Mater.* **2002**, *14*, 1706−1714.
(3) Khan, I. M.; Fish, D.; Delaviz, Y.; Smid, J. *Makromol. Chem.* **1989**, *190*, 1069−1078.
(4) Ruzette, A. G.; Soo, P. P.; Sadoway, D. R.; Mayes, A. M. *J. Electrochem. Soc.* **2001**, *148*, A537−A543.
(5) Matsen, M. W.; Bates, F. S. *Macromolecules* **1996**, *29*, 1091−1098.
(6) Khandpur, A. K.; Forster, S.; Bates, F. S.; Hamley, I. W.; Ryan, A. J.; Bras, W.; Almdal, K.; Mortensen, K. *Macromolecules* **1995**, *28*, 8796−8806.
(7) Bates, F. S.; Schulz, M. F.; Khandpur, A. K.; Forster, S.; Rosedale, J. H.; Almdal, K.; Mortensen, K. *Faraday Discuss. Chem. Soc.* **1995**, *98*, 7.
(8) Bailey, T. S.; Hardy, C. M.; Epps, T. H.; Bates, F. S. *Macromolecules* **2002**, *35*, 7007−7017.
(9) Lee, C. C.; Wright, P. V. *Polymer* **1982**, *23*, 681−689.

(10) Berthier, C.; Gorecki, W.; Minier, M.; Armand, M. B.; Chabagno, J. M.; Rigaud, P. *Solid State Ionics* **1983**, *11*, 91−95.
(11) Watanabe, M.; Nagano, S.; Sanui, K.; Ogata, N. *Solid State Ionics* **1986**, *18/19*, 338−342.
(12) Armand, M. *Annu. Rev. Mater. Sci.* **1986**, *16*, 245−261.
(13) Gray, F. M. *Solid Polymer Electrolytes, Fundamentals and Technological Applications*; VCH: Germany, 1991.
(14) Wolfenson, A. E.; Torresi, R. M.; Bonagamba, T. J.; De Paoli, M. A.; Panepucci, H. *J. Phys. Chem. B* **1997**, *101*, 3469−3473.
(15) Wieczorek, W.; Raducha, D.; Zalewska, A.; Stevens, J. R. *J. Phys. Chem. B* **1998**, *102*, 8725−8731.
(16) Andreev, Y. G.; Bruce, P. G. *Electrochim. Acta* **2000**, *45*, 1417−1423.
(17) Kim, Y. W.; Lee, W.; Choi, B. K. *Electrochim. Acta* **2000**, *45*, 1473−1477.
(18) Gadjourova, Z.; Andreev, Y. G.; Tunstall, D. P.; Bruce, P. G. *Nature (London)* **2001**, *412*, 520−523.
(19) Golodnitsky, D.; Livshits, E.; Rosenberg, Y.; Lapides, I.; Peled, E. *Solid State Ionics* **2002**, *147*, 265−273.
(20) Golodnitsky, D.; Peled, E. *Electrochim. Acta* **2000**, *45*, 1431−1436.
(21) Rangarajan, P.; Register, R. A.; Fetters, L. J. *Macromolecules* **1993**, *26*, 4640−4645.
(22) Quiram, D. J.; Register, R. A.; Marchand, G. R.; Ryan, A. J. *Macromolecules* **1997**, *30*, 8338−8343.
(23) Weimann, P. A. In *Chemical Engineering and Materials Science (Thesis)*; University of Minnesota: Minneapolis, 1998; p 218.
(24) Weimann, P. A.; Hajduk, D. A.; Chu, C.; Chaffin, K. A.; Brodil, J. C.; Bates, F. S. *J. Polym. Sci., Part B: Polym. Phys.* **1999**, *37*, 2053−2068.
(25) Chen, H. L.; Wu, J. C.; Lin, T. L.; Lin, J. S. *Macromolecules* **2001**, *34*, 6936−6944.
(26) Lee, W.; Chen, H.; Lin, T. *J. Polym. Sci., Part B: Polym. Phys.* **2002**, *40*, 519−529.
(27) Schmalz, H.; Knoll, A.; Muller, A. J.; Abetz, V. *Macromolecules* **2002**, *35*, 10004−10013.
(28) Floudas, G.; Vazaiou, B.; Schipper, F.; Ulrich, R.; Wiesner, U.; Iatrou, H.; Hadjichristidis, N. *Macromolecules* **2001**, *34*, 2947−2957.
(29) Hamley, I. W.; Castelletto, V.; Floudas, G.; Schipper, F. *Macromolecules* **2002**, *35*, 8839−8845.
(30) Fetters, L. J.; Lohse, D. J.; Ritcher, D.; Witten, T. A.; Zirkel, A. *Macromolecules* **1994**, *27*, 4639−4646.
(31) Robitaille, C. D.; Fauteux, D. *J. Electrochem. Soc.* **1986**, *133*, 315−325.
(32) Gorecki, W.; Belorizky, E.; Berthier, C.; Donoso, P.; Armand, M. *Electrochim. Acta* **1992**, *37*, 1685−1687.
(33) Chandrasekhar, V. *Adv. Polym. Sci.* **1998**, *135*, 139−205.
(34) Kato, Y.; Watanabe, M.; Sanui, K.; Ogata, N. *Solid State Ionics* **1990**, *40/41*, 632−636.
(35) Henderson, W. A. In *Chemical Engineering and Materials Science (Thesis)*; University of Minnesota: Minneapolis, 2002; p 180.
(36) Hiemenz, P. C. *Polymer Chemistry*; Marcel Dekker: New York, 1984.
(37) Young, R. J.; Lovell, P. A. *Introduction to Polymers*, 2nd ed.; Chapman & Hall: London, 1991.
(38) Jacobs, P. W. M.; Lorimer, J. W.; Russer, A.; Wasiucionek, M. *J. Power Sources* **1989**, *26*, 503−510.
(39) Semenov, A. N. *Sov. Phys. JETP* **1985**, *61*, 733.
(40) Semenov, A. N. *Macromolecules* **1989**, *22*, 2849−2851.
(41) Lipic, P. M.; Bates, F. S.; Matsen, M. W. *J. Polym. Sci., Part B: Polym. Phys.* **1999**, *37*, 2229−2238.
(42) Cochran, E. W.; Morse, D. C.; Bates, F. S. *Macromolecules* **2003**, *36*, 782−792.

MA021231O